Materials Chemistry and Physics 139 (2013) 931–935

Contents lists available at SciVerse ScienceDirect

Materials Chemistry and Physics

journal homepage: www.elsevier.com/locate/matchemphys

Mechanochemically assisted synthesis of nanocrystalline $BiFeO_3$

A.A. Cristóbal, P.M. Botta*

Instituto de Investigaciones en Ciencia y Tecnología de Materiales, INTEMA (CONICET-UNMdP), J.B Justo 4302, B7608FDQ Mar del Plata, Argentina

HIGHLIGHTS

- The mechanochemical reaction of $BiCl_3$, $FeCl_3$ and NaOH yields $BiFeO_3$ and NaCl.
- Heating at 600 °C improves the crystallization of the pure ferrite phase.
- NaCl byproduct is removed by washing of the calcined powder.
- $BiFeO_3$ powder consists of particles of 100 nm formed by crystals of 30 nm.
- Magnetic and electric transitions are determined by thermal analyses.

ARTICLE INFO

Article history:
Received 11 September 2012
Received in revised form
15 February 2013
Accepted 17 February 2013

Keywords:
Inorganic compounds
Magnetic materials
Powder diffraction

ABSTRACT

The synthesis of multiferroic $BiFeO_3$ phase is carried out by means of a solid-state reaction induced by high energy ball-milling between metal chlorides (Lewis' acids) and sodium hydroxide (base). The chemical reaction occurs at room temperature and produces a solid mixture of nanocrystalline $BiFeO_3$ and NaCl. Thermal treatments at several temperatures are performed to favor the crystallization of the desired phase. The evolution of the mechanochemical reaction and calcination are followed by X-ray diffraction, Raman spectroscopy and scanning electron microscopy. Electric and magnetic ordering transitions are determined by thermal analysis.

1. Introduction

Multiferroics can be formally defined as materials that display simultaneously two or more primary ferroic orderings [1,2]. These orderings refer to ferromagnetism, ferroelasticity and ferroelectricity. When a ferromagnetic order is induced by an electric field and/or ferroelectric polarization is achieved by the action of a magnetic field, the effect is so-called magnetoelectric. This is the result of the coupling of both ferroelectric (FE) and ferromagnetic (FM) orderings and they can find interesting applications, such as high-storage density media and high-sensitive sensors for magnetic fields [3]. Unfortunately the coexistence between FE and FM in a single solid structure is very rare, because the conventional FE state (off-centering of a transition-metal cation driven by the hybridization with its surroundings anions) is disfavored if the cation is magnetic with a partially filled *d* shell [4]. $BiFeO_3$ is a well-known compound where both ferroic orderings combine. Its crystal structure at room temperature is a rhombohedrally distorted perovskite. Bismuth cation (A site) contains a lone electron pair, giving rise to a ferroelectric polarization along the [111] direction, with a $T_C = 1123$ K. The magnetic structure consists in a G-type antiferromagnetic ordering ($T_N = 643$ K) with each ferric ion surrounded by six canted antiparallel spins, that produce a small net magnetic moment [5,6].

The preparation of pure $BiFeO_3$ is often problematic because of the narrow interval of thermal stability of this phase and the formation of secondary phases, such as $Bi_{25}FeO_{40}$ and $Bi_2Fe_4O_9$ [7,8]. Several methods, including solid-state reaction, sol–gel and hydrothermal synthesis have been used with diverse results [9–12].

High-energy milling of solids can increase the chemical reactivity in a significant way, producing in some cases solid-state reactions at room temperatures (mechanochemical reactions), or the decrease of the reaction temperature in a subsequent thermal treatment [13]. This methodology has been employed in the last decades for obtaining a variety of materials with special properties [14–16]. There are a few previous reports where mechanochemical activation was used for preparing $BiFeO_3$ [17–20]. In all the cases the traditional methodology was used, starting from Fe_2O_3 and

* Corresponding author. Tel.: +54 2234816600; fax: +54 2234810046.
E-mail address: pbotta@fi.mdp.edu.ar (P.M. Botta).

0254-0584/$ – see front matter © 2013 Elsevier B.V. All rights reserved.
http://dx.doi.org/10.1016/j.matchemphys.2013.02.058

Bi_2O_3 and milling for prolonged times (in some cases longer than 24 h). In the present paper we reintroduce an interesting alternative route for obtaining inorganic nanocrystalline particles developed by McCormick et al. [21,22]. The method consists in producing a mechanochemical reaction between an acid (metallic salt) and a base (usually an alkaline oxide or hydroxide). In this reaction a metallic oxide is formed together with a byproduct, which is a very soluble salt. In the first stages, the mechanical action produces a succession of events of fracture and welding of the powder particles, leading to its plastic deformation and the generation of subcrystallites [23]. As the milling time increases, the sub-crystallite size decreases, reaching nanometric dimensions. This very small crystallite size accelerates the acid–base reaction, favoring its occurrence at room temperature. The product phase crystals reproduce the nanometric dimensions of the milled reactants, forming a composite solid, in which each oxide nanoparticle is surrounded by the soluble salt phase [21]. After washing, the byproduct is removed and a powder oxide with separated nanoparticles is obtained. This method was employed to prepare a variety of single oxides, such as Al_2O_3, ZrO_2, CeO_2, Fe_2O_3, etc [24–27]. However its application to the synthesis of mixed oxides is very uncommon [28].

In this work we investigate this alternative mechanochemical route to prepare the multiferroic perovskite $BiFeO_3$, focusing on its physicochemical properties and microstructure.

2. Experimental

2.1. Preparation of samples

Starting materials were $BiCl_3$ (commercial reagent, ≥98 wt%), $FeCl_3 \cdot 6H_2O$ (commercial reagent, 99 wt%) and NaOH (commercial reagent, 98 wt%). These reagents were mixed in the stoichiometric ratio necessary for obtaining $BiFeO_3$.

A planetary laboratory ball-mill (Fritsch Pulverisette 7) with vials and balls made of WC was used for the mechanochemical treatments of the reactive mixture. The milling vials were loaded with 5 g of powder mixture and 4 balls of 15 mm diameter each, resulting in a ball-to-powder mass ratio of 22. The vials were rotated at 1500 rpm under air atmosphere during different times. The obtained samples were labeled BFO*x*, where *x* is the activation time in hours.

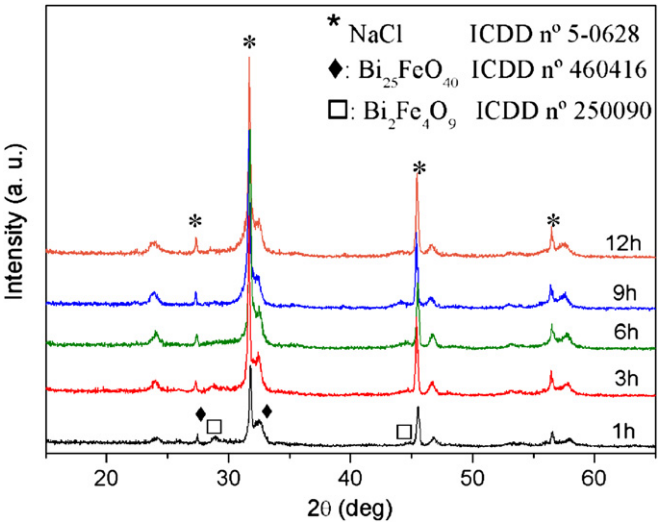

Fig. 1. XRD patterns of the reactive powders activated between 1 and 12 h. Unmarked peaks correspond to $BiFeO_3$ phase (ICDD n°74-2016).

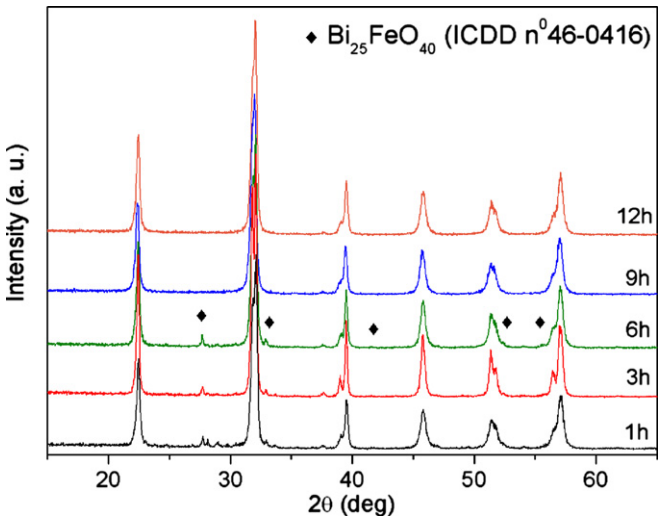

Fig. 2. XRD patterns of samples activated for different times, then heated at 600 °C and washed.

The activated samples were thermally treated during 1 h under air atmosphere at temperatures ranging from 400 to 700 °C. These milled and calcined powders were called BFO*x*-*y* being *y* the temperature of the thermal treatment in Celsius degrees.

The activated and calcined samples were washed by stirring with distilled water to remove the NaCl formed as secondary product of reaction. The decanted solids were filtered and dried at 60 °C for several hours.

2.2. Characterization

Crystalline phases were characterized by X-ray diffraction (XRD) using an X'Pert PRO PANalytical diffractometer, equipped with a graphite monochromator, using CuKα radiation (λ = 1.5406 Å) at 40 kV and 40 mA. All the diffractograms were scanned between 15° and 65° 2θ with a step size of 0.02°.

The microstructure of the samples was examined in a scanning electron microscope (SEM) Philips 505. Prior to the observations, the samples were sputtered with gold.

Differential thermal analyses (DTA) were performed in a Shimadzu DTA-50H instrument under flowing synthetic air, using a

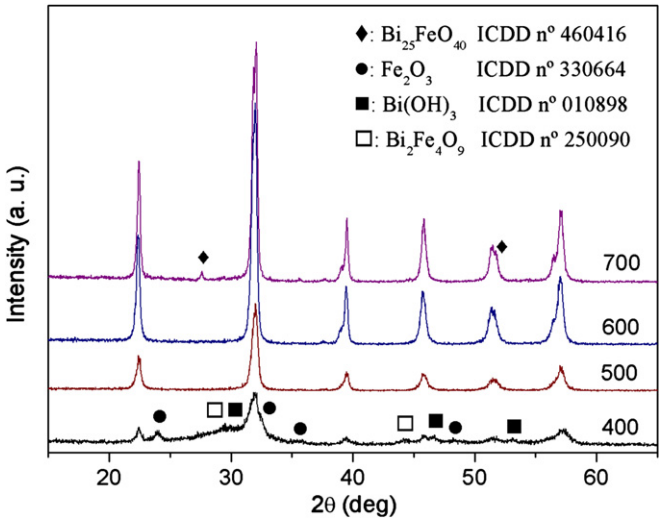

Fig. 3. XRD diagrams of the reactive powder milled for 9 h, then heated at several temperatures and washed.

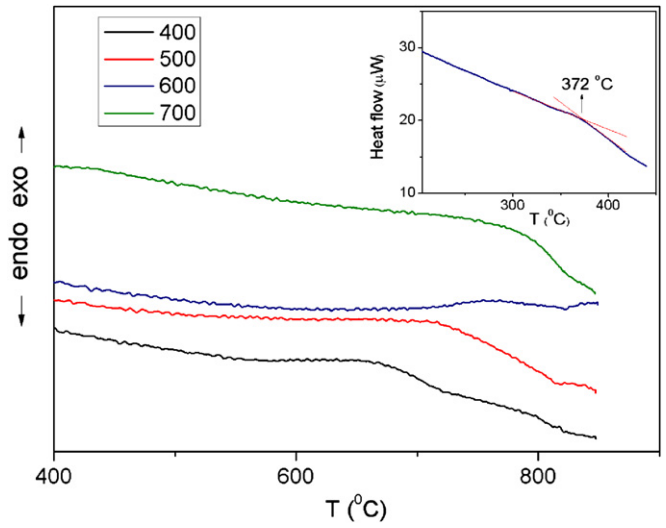

Fig. 4. DTA curves of sample BFO9 calcined at several temperatures. The inset shows a DSC scan of sample BFO9-600 (the straight lines are drawn to evidence the slope change).

heating rate of 10 °C min^{-1} and approximately 40 mg of sample mass. Also a Shimadzu DSC-50 differential scanning calorimeter (DSC) was used to study the thermal behavior of samples between room temperature and 450 °C. A heating rate of 10 °C min^{-1} and approximately 20 mg of sample were used.

Raman spectroscopy was performed at room temperature using an Invia Reflex confocal Raman microprobe with Ar^{+} laser of 514 nm in backscattering mode, with a laser spot of 10 μm. An exposure time of 20 s and 3 accumulations were used, with 50× objective. The laser power was reduced to 10% to prevent damage by heating (0.2 mW).

3. Results and discussion

Fig. 1 shows the evolution of XRD patterns of samples BFO with the activation time.

From 1 h on the complete absence of reactants and the appearance of broad peaks corresponding to $BiFeO_3$ can be noticed. Also very intense and narrow peaks corresponding to NaCl are observed, which indicates that the reaction (1) is taking place into the milling bowls, already at the first stages of the mechanical treatment:

$$FeCl_3 + BiCl_3 + 6NaOH \rightarrow BiFeO_3 + 3H_2O + 6NaCl \quad (1)$$

Moreover small peaks corresponding to impurity phases such as $Bi_2Fe_4O_9$ and $Bi_{25}FeO_{40}$ can be noticed. There are not significant changes in the diffractograms registered for different activation times.

In Fig. 2 XRD patterns of the activated samples calcined at 600 °C are shown. In samples activated during less than 9 h peaks corresponding to the phase $Bi_2Fe_4O_9$ appear. This impurity phase is detected in very small proportion and is not further observed for activation times longer than 9 h.

Crystallite size for the samples BFO*x*-600 was determined by the Scherrer equation [29]. This calculation gave approximately 23 nm for all the activation times. The nanometric size obtained is a consequence of the restricted grain growth provoked by the continuous process of fracture and welding of reactant particles during the mechanical treatment [21].

Fig. 3 shows XRD diagram of sample BFO9 annealed at different temperatures. As temperature increases a continuous refinement of the orthoferrite crystalline structure can be observed. As expected, the point and surface defects accumulated in the powder during the activation were healed by effect of thermal energy.

XRD diagram of sample BFO9-600 reveals the presence of well-crystallized $BiFeO_3$ as the only component of these powders.

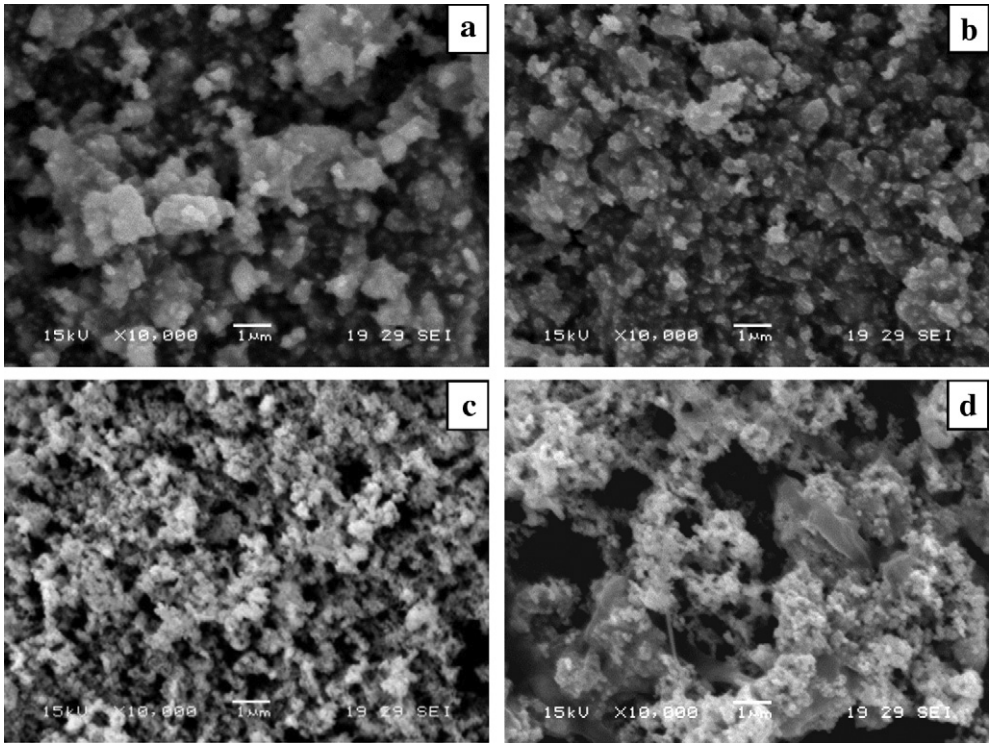

Fig. 5. SEM images of sample BFO9 heated at 400 °C (a), 500 °C (b) and 600 °C (c), after washing. Micrograph (d) corresponds to the unwashed powder BFO9-600.

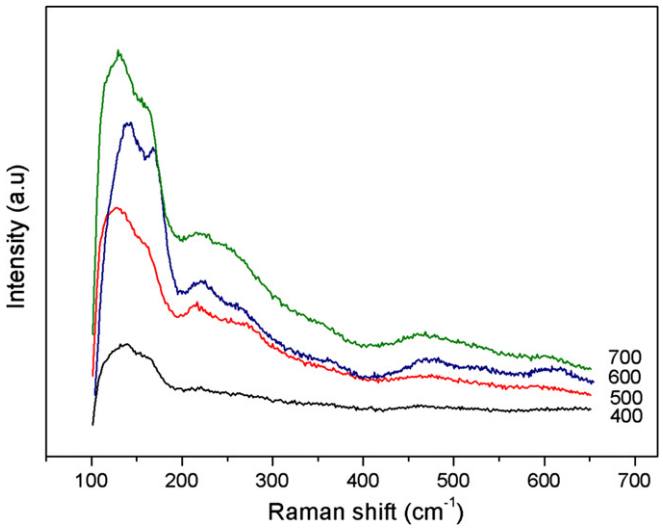

Fig. 6. Raman spectra of sample BFO9 calcined at several temperatures and washed.

However at 700 °C a small peak corresponding to the secondary phase $Bi_{25}FeO_{40}$ can be seen, indicating that to this temperature $BiFeO_3$ is decomposing. Although the compositional phase diagram of $BiFeO_3$ shows stability for this solid until 950 °C (melting point), there is experimental evidence that indicates that some impurities nucleate into the grain boundaries [7]. In fact some authors consider $BiFeO_3$ as a metastable phase in air, which contains small inclusions of spurious phases at temperatures quite lower than melting point [30]. Crystallite sizes of $BiFeO_3$ for calcined samples are ranged from 29 nm to 37 nm for samples heated between 400 and 700 °C, respectively.

Fig. 4 displays DTA scans for the samples BFO9-*y*. At about 820 °C an endothermic broad peak is observed in all the curves. This event corresponds to the structural transformation of low-temperature rhombohedral $BiFeO_3$ to a centrosymmetric high-temperature structure. A peak in dielectric constant has been reported at about this temperature, which suggests the existence of a ferroelectric–paraelectric transition [31], in agreement with the change of structural symmetry. The DTA peak can be more clearly observed for samples calcined at 500 and 600 °C. According to XRD results (Fig. 3), $BiFeO_3$ is not well crystallized at 400 °C and it starts to decompose at 700 °C. The inset of Fig. 4 shows the DSC curve for the most pure sample, BFO9-600. A change in the curve slope at 372 °C can be observed, which is attributed to the Néel (antiferromagnetic-paramagnetic) transition [32].

SEM images of samples BH9-y are shown in Fig. 5. In the washed powder calcined at 400 °C micrometric agglomerates of irregular particles can be observed. As temperature increases the particle shape is more defined and the agglomeration diminishes. Washed sample BH9-600 (Fig. 5c) consists of rounded particles with an average diameter about 100 nm. Fig. 5d shows an image of sample BH9-600 before washing, in which big particles (4–5 microns) are surrounded by particles with nanometric sizes. The comparison with Fig. 5c suggests that micrometric particles are NaCl, which are completely removed after washing with distilled water. The large size of the by-product crystals observed by SEM is consistent with XRD results (Fig. 1), where very narrow peaks corresponding to NaCl are observed from 1 h of milling on.

Fig. 6 displays Raman spectra for the powders activated for 9 h and heated at different temperatures. It can be observed for all the curves that each peak corresponds to different vibrational modes of $BiFeO_3$ phase, three A_1 modes (approximately at 132, 168 and 220 cm^{-1}) and three *E* modes (at approximately 268, 362 and 473 cm^{-1}). These positions are somewhat different from those previously reported for this compound [11,33]. Taking into account that the Raman signals reflect the vibration frequencies of oxygen and metallic atoms, these differences could be attributed to the structural disorder produced by the mechanical treatment. Peaks belonging to other phases are not observed.

According to the results obtained by the characterization we can conclude that the optimal synthesis condition to obtain pure nanocrystalline $BiFeO_3$ consists in a ball-milling of the reactants by 9 h followed by a thermal treatment for 1 h at 600 °C and a final washing to remove NaCl byproduct.

4. Conclusions

Mechanochemical activation of iron and bismuth chlorides with sodium hydroxide produces a chemical reaction with formation of $BiFeO_3$ and NaCl. Although this reaction takes place at very short milling times, longer times are required in order to obtain $BiFeO_3$ free of $Bi_2Fe_4O_9$ and $Bi_{25}FeO_{40}$ impurities. A better crystallization is achieved after heating the milled powder at 600 °C. The pure $BiFeO_3$ phase is obtained after washing the calcined powder to remove the saline byproduct. The final material consists in particles with mean size of about 100 nm constituted by crystallites of approximately 30 nm in diameter. Electric and magnetic ordering transitions were detected at 820 °C and 372 °C, respectively, in very good agreement with previously reported values. The synthesis investigated in this work results interesting since it allows producing nanocrystalline pure $BiFeO_3$ in a relatively large scale and using a procedure completely free of organic reactants and solvents.

Acknowledgments

The authors gratefully thank CONICET, UNMdP and ANPCyT for the financial support given to this work.

References

[1] W. Eerenstein, N.D. Mathur, J.F. Scott, Nature 442 (2006) 759–765.
[2] C.A.F. Vaz, J. Hoffman, C.H. Ahn, R. Ramesh, Adv. Mater. 22 (2010) 2900–2918.
[3] J. Ma, J. Hu, Z. Li, C.W. Nan, Adv. Mater. 23 (2011) 1062–1087.
[4] N.A. Hill, J. Phys. Chem. B 104 (2000) 6694–6709.
[5] G. Catalan, J.F. Scott, Adv. Mater. 21 (2009) 2463–2485.
[6] S.M. Selbach, T. Tybell, M.-A. Einarsrud, T. Grande, J. Solid State Chem. 183 (2010) 1205–1208.
[7] M. Valant, A.-K. Axelsson, N. Alford, Chem. Mater. 19 (2007) 5431–5436.
[8] T.T. Carvalho, P.B. Tavares, Mater. Lett. 62 (2008) 3984–3986.
[9] S.M. Selbach, T. Tybell, M.-A. Einarsrud, T. Grande, Chem. Mater. 21 (2009) 5176–5186.
[10] J.K. Kim, S.S. Kim, W.-J. Kim, Mater. Lett. 59 (2005) 4006–4009.
[11] H. Zhang, K. Kajiyoshi, J. Am. Ceram. Soc. 93 (2010) 3842–3849.
[12] A.K. Pradhan, K. Zhang, D. Hunter, J.B. Dadson, G.B. Loutts, J. Appl. Phys. 97 (2005) 093903.
[13] S.L. James, C.J. Adams, C. Bolm, D. Braga, P. Collier, T. Friščić, et al., Chem. Soc. Rev. 41 (2012) 413–447.
[14] V. Šepelák, Ann. Chim. Sci. Mater. 27 (2002) 61–76.
[15] D.L. Zhang, Prog. Mater. Sci. 49 (2004) 537–560.
[16] F. Delogu, G. Mulas, Experimental and Theoretical Studies in Modern Mechanochemistry, Transworld Research Network, Kerala, 2010.
[17] I. Szafraniak, M. Połomska, B. Hilczer, A. Pietraszko, L. Kepiński, J. Eur. Ceram. Soc. 27 (2007) 4399–4402.
[18] D. Maurya, H. Thota, K. Singh Nalwa, A. Garg, J. Alloys Compd. 477 (2009) 780–784.
[19] K.L. Da Silva, D. Menzel, A. Feldhoff, C. Kel, M. Bruns, A. Paesano, et al., J. Phys. Chem. C 115 (2011) 7209–7217.
[20] C. Correas, T. Hungría, A. Castro, J. Mater. Chem. 21 (2011) 3125–3132.
[21] P.G. McCormick, T. Tsuzuki, J.S. Robinson, J. Ding, Adv. Mater. 13 (2001) 1008–1010.
[22] T. Tsuzuki, P.G. McCormick, J. Mater. Sci. 39 (2004) 5143–5146.
[23] H. Yang, P.G. McCormick, Metall. Mater. Trans. B 29 (1998) 449–455.
[24] J. Ding, T. Tsuzuki, P.G. McCormick, R. Street, J. Am. Ceram. Soc. 79 (1996) 2956–2958.
[25] A.C. Dood, T. Tsuzuki, P.G. McCormick, Mater. Sci. Eng. A 301 (2001) 54–58.
[26] T. Tsuzuki, P.G. McCormick, J. Am. Ceram. Soc. 84 (2001) 1453–1458.

[27] J. Ding, T. Tsuzuki, P.G. McCormick, Nanostr. Mater. 8 (1997) 75–81.
[28] M. Muroi, P.G. McCormick, R. Street, Rev. Adv. Mater. Sci. 5 (2003) 76–81.
[29] B.D. Cullity, Elements of X-ray Diffraction, second ed., Addison-Wesley Publ. Co., Reading, 1976.
[30] R. Palai, R.S. Katiyar, H. Schmid, P. Tissot, S.J. Clark, J. Robertson, S.A.T. Redfern, G. Catalan, J.F. Scott, Phys. Rev. B 77 (2008) 014110.
[31] R. Haumont, I.A. Kornev, S. Lisenkov, L. Bellaiche, J. Kreisel, B. Dkhil, Phys. Rev. B 78 (2008) 134108.
[32] G.A. Smolenskii, V.M. Yudin, E.S. Sher, Y.E. Stolypin, Sov. Phys. JETP 16 (1963) 622–624.
[33] D. Kothari, V. Raghavendra Reddy, V.G. Sathe, A. Gupta, A. Banerjee, A.M. Awasthi, J. Magn. Magn. Mater. 320 (2008) 548–552.